Langmuir

Article

pubs.acs.org/Langmuir

Electrowetting-Induced Droplet Detachment from Hydrophobic Surfaces

Seung Jun Lee,[†,‡] Jiwoo Hong,[†,‡] Kwan Hyoung Kang,[‡] In Seok Kang,*[,§] and Sang Joon Lee*[,‡]

[‡]Department of Mechanical Engineering, Pohang University of Science and Technology (POSTECH), San 31, Hyoja-dong, Pohang 790-784, South Korea

[§]Department of Chemical Engineering, Pohang University of Science and Technology (POSTECH), San 31, Hyoja-dong, Pohang 790-784, South Korea

Supporting Information

ABSTRACT: Detachment of droplets from solid surfaces is a basic and crucial process in practical applications such as heat transfer and digital microfluidics. In this study, electrowetting actuations with square pulse signals are employed to detach droplets from a hydrophobic surface. The threshold voltage for droplet detachment is obtained both experimentally and theoretically to find that it is almost constant for various droplet volumes ranging from 0.4 to 10 μL. It is also found that droplets can be detached more easily when the width of applied pulse is well-matched to the spreading time (i.e., the time to reach the maximum spread diameter). When the droplet is actuated by a double square pulse, the threshold voltage is reduced by ~20% from that for a single square pulse actuation. Finally, by introducing an interdigitated electrode system, it is demonstrated that droplets can be detached from the solid bottom surface without using a top needle electrode.

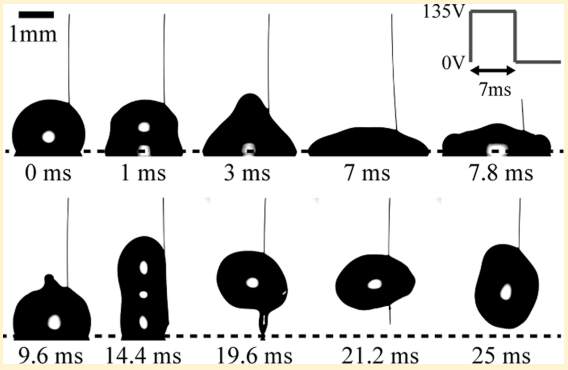

1. INTRODUCTION

The detachment (or removal) of droplets from a solid surface is one of the essential processes in various practical applications, such as heat transfer,[1−4] fuel cells,[5] wiperless windows,[6] soft printing,[7] and droplet-based microfluidics.[8−11] For example, in the condensation processes of phase-change heat transfer, large-scale condensate drops formed on a solid surface reduce the contact area for heat exchange between the solid surface and the vapor and act as a thermal resistance between them.[12] Therefore, the effective removal of such drops from a solid surface can improve the heat transfer rate. In addition, digital microfluidics (DMF), which is a technology to manipulate discrete droplets on an array of electrodes by means of dielectrophoresis (DEP) or electrowetting (EW),[13] have problems such as solute adsorption and cross-contamination because droplets contact and move on solid substrates.[14] To improve throughput for analysis and device integration as well as to address these issues, three-dimensional (3-D) DMF have been proposed.[15−17] In 3-D DMF, detachment of droplets from solid surfaces is one of the most salient processes.

To detach a droplet from a solid surface, the applied external force should be larger than the threshold force of the droplet adhered on the solid surface. To this end, a mechanical vibration method has been developed.[1,18] Droplets are detached from solid surfaces when the surfaces are vibrated at resonant frequencies of the droplets with minimum forcing acceleration of ~10g.[1]

At high forcing acceleration (~400g) with a frequency of ~1 kHz, droplets are atomized and removed.[18] However, the mechanical moving parts cause several problems, such as noise generation and difficulties in integration. Alternatively, droplets have been detached from a solid surface by electrostatic forces.[19,20] A vertical electrostatic force can induce sessile droplets to lift toward the upper substrate. However, high voltage (~a few kV) and high electric field (~MVm^{-1}) are required in this approach even if droplets sit on superhydrophobic surfaces in air or on hydrophobic surfaces in oil to minimize the contact area between the droplets and the solid surface.

Recently, EW has been used for detaching or removing droplets from solid surfaces.[16,21] EW electrically controls the wettability of a droplet on the substrate and has several advantages such as fast response, low driving voltage, and absence of mechanically moving parts.[22,23] Owing to the extraordinary features of low adhesion and drag reduction, EW on superhydrophobic surfaces has attracted increasing attention with the advances in fabrication techniques.[24−27] Recently, we observed that a droplet can be continuously bounced on the superhydrophobic surface by using AC EW at the resonance frequency.[21] We also reported that a droplet can jump on the

Received: November 9, 2013
Revised: January 28, 2014
Published: February 3, 2014

superhydrophobic surface under EW actuations with the square pulse as well as the sinusoidal pulse.[16] More recently, Lapierre et al. demonstrated that a droplet can be bounced on the superhydrophobic surface by applying an AC modulated signal.[27]

However, hydrophobic surfaces such as Teflon (DuPont Co.)-coated surfaces have been conventionally employed for diverse EW-based applications rather than superhydrophobic surfaces. In addition, for construction of 3-D DMF platforms, the detached droplet from the bottom plate should be attached to the top plate, and then the hanging droplet should be transported horizontally along the top plate. However, it is difficult to perform these processes on both top and bottom plates with superhydrophobic surfaces. Accordingly, we need to extend previous research studies on the droplet jumping on superhydrophobic surfaces[16,21,27] by demonstrating EW-induced droplet detachment from a hydrophobic surface under the applied square pulse. The effects of the applied voltage on the spreading, receding, and jumping behaviors of electrowetted droplets are investigated. Then, the threshold voltage is experimentally and theoretically determined with a focus on how to reduce it for practical applications. The effect of the pulse width of electrical signal on the droplet detachment is also experimentally investigated. Finally, we examine the droplet detachment from a hydrophobic surface using two interdigitated electrodes instead of a top needle electrode.

2. EXPERIMENTAL SETUP

The experimental setup is similar to the conventional EW experiment, as shown in Figure 1.[23] An indium−tin-oxide (ITO)-coated glass was used as a base material and coated with a parylene-C layer of 5.0 ± 0.2 μm thickness as an insulating layer (Figure 1a). A Teflon AF 1600 layer of ∼100 nm thickness was spin-coated on the top of it to make a hydrophobic surface. An aqueous 1 mM NaCl solution was used as the conducting liquid. A droplet was dispensed using a micropipet, and its volume ranged from 0.4 to 10 μL. The measurement uncertainties in the droplet volume data were ±0.1 μL. The static contact angle of the sessile droplets was 116° ± 3°, and the advancing and receding contact angles were 119° ± 3° and 110° ± 3°, respectively.[28] A tungsten wire of 25 μm in diameter was immersed in the test droplet as a top electrode. It was not coated with any hydrophobic or hydrophilic layer. The diameter of the needle electrode was ∼2% of the base diameter of a 5 μL droplet. Because the capillary force exerted on the droplet is proportional to the contact length, we can conjecture that the needle electrode has negligible influence on the droplet motion. An electrical signal of square pulse waves generated by a function generator (33220 A, Agilent) was amplified 100 times with an amplifier (A800, FLC). An electric voltage with a peak value of 90 V_{pp} to 240 V_{pp} and a pulse width (T_p) of 2−10 ms was applied to the test droplet. Throughout this study, the applied voltages represent the peak-to-peak voltage.

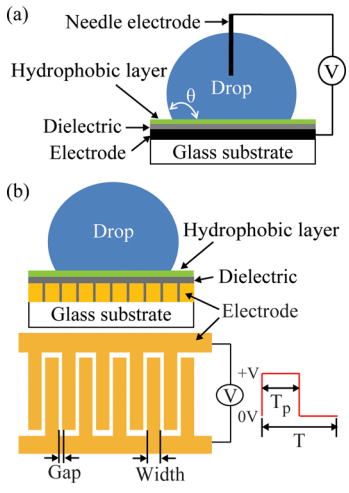

Figure 1. Experimental setups. (a) ITO glass substrate (bottom) and needle electrode (top) were used to apply electric voltage to a droplet. (b) Two interdigitated comb-shape electrodes were used to apply electric voltage to a droplet without a top needle electrode. In both experimental setups (a) and (b), a square pulse voltage was applied to the test droplet. T and T_p denote the period of the square pulse wave and the pulse width at high voltage (+V), respectively.

To demonstrate droplet detachment without using needle electrodes, two interdigitated comb-shape electrodes were utilized (Figure 1b).[29,30] The electrodes were fabricated as follow. Aluminum (200 nm ± 10 nm thickness) was deposited on a glass wafer using an e-beam evaporator, and then a photoresist (AZ 5214, AZ Electronic Materials) was patterned using photolithography. The deposited aluminum was wet-etched to form combs with widths of 100 μm, with a 20 μm gap between two adjacent electrodes. After removing the remaining photoresist, an insulating layer of parylene-C (2.6 ± 0.1 μm thick) was vapor-deposited using a parylene coating system. A layer of Teflon AF1600 (DuPont, 100 nm thickness) was spin-coated on the top of the insulation layer.

Images of a droplet detaching from the hydrophobic surface were consecutively recorded at 5 000 frames per second (fps) using a high-speed camera (Fastcam SA3, Photron). A long-distance zoom lens (Zoom 70XL, OPTEM) was attached in front of the camera. MATLAB was employed in the digital image processing and data analysis to obtain the variations of the base radius, apex height, and jumping height of droplets. To determine the jumping heights (H_{cm}), the distance between the centroid positions of the maximum stretched droplets and airborne droplets was measured, assuming that the droplets have axis-symmetric shapes. Every experiment was repeated at least three times with new droplets. Each experiment was completed within 2 min to avoid any evaporation effect.

3. RESULTS AND DISCUSSION

The detaching process (i.e., spreading, receding, and jumping) of a 5 μL sessile droplet from the hydrophobic surface by applying one square pulse voltage between ITO and needle electrodes was consecutively captured (Figure 2a). The temporal variations of base radius and apex height at various applied voltages were quantitatively analyzed (Figure 2b). Here, the pulse width (T_p) of the applied square pulse voltage was determined based on the results of a preliminary experiment on droplet spreading with applying DC voltage. The spreading time (T_s, i.e., time to reach the maximum spread diameter) of a droplet was nearly constant (∼7 ms), regardless of the applied DC voltage.[28] To interrupt the electric power supply after the droplet reaches the maximum wetted radius, the condition of $T_p = T_s = 7$ ms was selected for the 5 μL droplets tested in this study. Accordingly, the electrical force is negligible in the droplet receding phase. The effects of the pulse width on droplet detachment will be discussed in detail later.

When a voltage of 135 V with $T_p = 7$ ms is applied, EW actuation induces drop spreading and capillary waves along the droplet surface (Figure 2a). The droplet spreads to the maximum spread diameter (∼7 ms), enabling it to store a large amount of surface energy. When the maximum wetted droplet is released, the base radius of the droplet decreases sharply until it reaches the initial base radius (Figure 2b). As shown in parts a and b of Figure 2, the shape of the receding droplet at $t = 9.6$ ms is similar to that of the initial droplet at $t = 0$ ms. Thereafter, the receding velocity of the base radius decreases gradually, and the apex of the droplet reaches the

dx.doi.org/10.1021/la404344y | Langmuir 2014, 30, 1805−1811

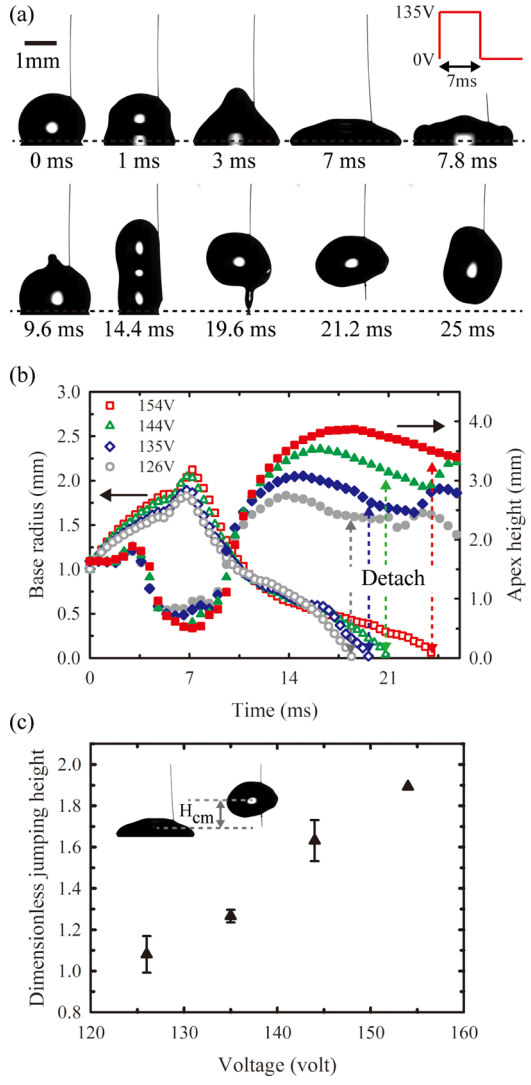

Figure 2. Spreading, receding, and jumping dynamics of a 5 μL droplet. (a) Temporal evolution of detachment process of a 5 μL droplet from a hydrophobic surface at 135 V_{pp} with a square pulse of T_p = 7 ms (diamond symbol in (b)). The dotted lines indicate the contact surface of the droplet. (b) Temporal variations of base radius (open symbols) and apex height (filled symbols) under various applied voltages. The dashed arrow denotes the instance of droplet detachment at each voltage. (c) Variation of dimensionless jumping height (H_{cm}/R) according to the applied voltage. H_{cm} is the vertical height between the centroids of the maximum spread droplet and the airborne droplet. R is the radius of a spherical droplet of the same volume. The error bar denotes the standard deviation between test cases at the same voltage. The spatial resolution of the imaging system is that one pixel corresponds to ~8.7 μm.

maximum height at t = 14.4 ms (Figure 2a and b). In the receding process, the surface energy of the droplet stretched with maximum diameter is mainly converted to kinetic energy, and then this kinetic energy induces vertical elongation. Finally, the receding droplet is detached from the substrate under certain conditions. The threshold conditions will be discussed in detail in the succeeding sections. Figure 2c shows that the jumping height of a droplet increases with the applied voltage. The jumping height (H_{cm}) is nondimensionalized by the radius of a spherical droplet of the same volume, $R = (3\Delta/4\pi)^{1/3}$, where Δ is its volume. When the dimensionless jumping height (H_{cm}/R) is >1, the droplet can take off from the solid surface. As the applied voltage increases, the maximum base radius and the surface energy of the maximally stretched droplet also increase (Figure 2b). That is, the droplet with large surface energy can be detached from the substrate and jumps higher than that with a low surface energy. The threshold voltage of a 5 μL droplet is about 126 V. Here, the threshold voltage is defined as the minimum voltage required to detach the droplet from the solid surface (i.e., $H_{cm}/R > 1$).

As the applied voltage increases to 154 V, the maximum jumping height of a 5 μL droplet increases to about 2R. The results for 0.4 μL droplets are shown in Figure S1 of the Supporting Information.

To investigate the effect of pulse width T_p on droplet detachment, the minimum and maximum pulse widths of detaching droplets were measured with varying T_p at fixed T_s for different EW numbers $\eta = \varepsilon\varepsilon_o V^2/2d\gamma$. The EW number represents the ratio of the electrical force to the surface tension force. Here ε is the dielectric constant of insulator, ε_o is the vacuum dielectric permittivity, V is the applied voltage, d is the thickness of the insulator, and γ is the surface tension of liquid. As the EW number increases, the minimum pulse width for droplet detachment ($T_{p,min}$) decreases and the maximum pulse width ($T_{p,max}$) increases. Both pulse widths are then almost saturated at a high EW number of η = 1.0. This result indicates that when T_p is longer than $T_{p,max}$ or shorter than $T_{p,min}$ droplets cannot be detached, even though the EW number is sufficiently large. Finally, the maximum and minimum values of T_p for droplet detachment ($T_{p,max}$ and $T_{p,min}$, respectively) are related to the threshold position of the contact line for detaching droplet.

The minimum and maximum values of the nondimensional pulse width (T_p/T_s) for droplet detachment are in the range of 0.5−1.5 at η = 0.79 for 5 μL droplets (Figure 3b and c). This tendency is also observed at η = 0.90 for 0.4 μL droplets (Figure 3a). From these results, we can see that a droplet can be detached from the substrate by suitably tuning the pulse width of square pulse actuation. Interestingly, a very tiny droplet is ejected from the apex of the droplet at η = 0.79 with T_p/T_s = 0.5 (Figure 3c). Just before the ejection, the droplet has a doughnut-like shape at t = 4.8 ms. Thereafter, the liquid jet is ejected from the apex at t = 6.4 ms, which is quite similar to the liquid jet observed in a previous study on droplet impact.[31]

A relationship between droplet volume and threshold voltage (or EW number) was established. Here, the threshold voltage denotes the minimum electrostatic energy required for droplet detachment (Figure 4a). Measured T_s for each droplet volume are T_s = 2 ms (0.4 μL), 3 ms (1 μL), 5.3 ms (3 μL), 7 ms (5 μL), and 9 ms (10 μL). When the droplet volumes are 3, 5, and 10 μL, the average threshold value of EW number η is ~0.79 (~130 V). As the droplet volume decreases from 10 to 0.4 μL, the average threshold (η_{avg}) is increased slightly by $\Delta\eta_{avg}$ = ~0.05 (~5 V). Although the threshold value for each droplet volume is slightly different, all of them are within the range of η = 0.60−0.75 (125−140 V). Consequently, the threshold voltage is rarely affected by droplet volume. We compared the experimentally measured threshold values with the theoretical one derived by using energy balance between the electrical energy and adhesion work, which will be described in the succeeding sections.

When a single square pulse is applied, the threshold voltage for droplet detachment is high (125−140 V, corresponding to η = 0.60−0.75). This threshold voltage is close to the saturation

dx.doi.org/10.1021/la404344y | Langmuir 2014, 30, 1805−1811

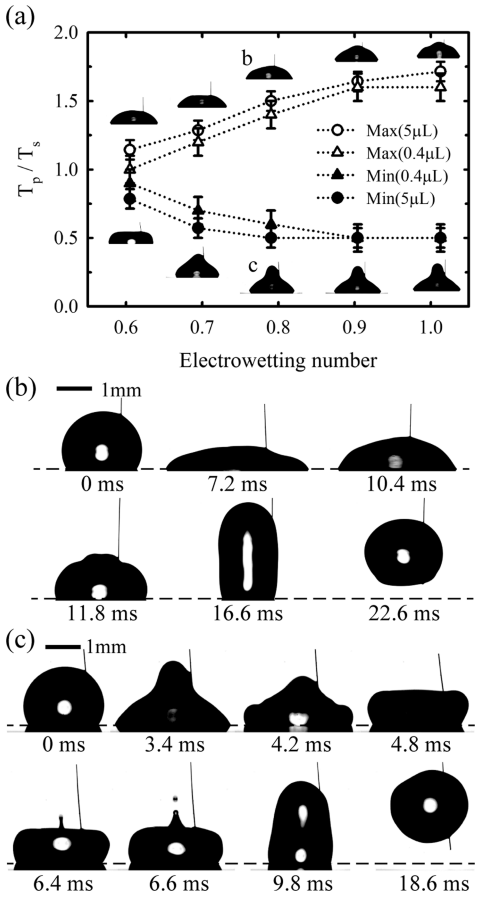

Figure 3. (a) Variations of nondimensionalized maximum and minimum pulse widths (T_p/T_s) of detaching droplets with respect to electrowetting number (η). Side-view images of the spread droplets were captured just before the applied voltage is turned off at each condition. The error bar denotes the standard deviation of the test cases at the same η. (b) Consecutive side-view images of a 5 μL droplet detached at η = 0.79 with T_p/T_s = 1.5 (T_p = 10.5 ms) (image b in (a)). (c) Consecutive side-view images of a 5 μL droplet detached at η = 0.79 with T_p/T_s = 0.5 (T_p = 3.5 ms) (image c in (a)). Before detaching from the substrate, a small droplet is ejected from the apex of the droplet. In (b) and (c), the dotted lines indicate the contact surface of the droplet.

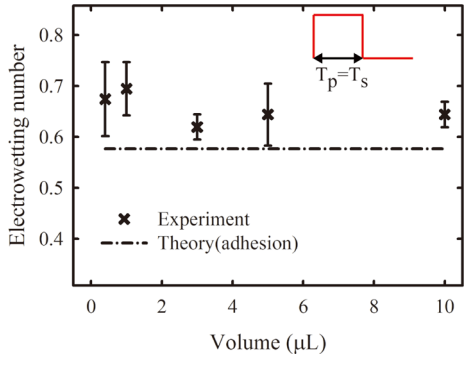

Figure 4. Variation of threshold electrowetting number for droplet detachment with respect to different droplet volumes under single square pulse actuation with $T_p = T_s$. Experimental results are compared with the theoretical ones.

voltage (140−160 V) where contact angle becomes saturated.[32] To reduce the threshold voltage, we utilized the double square pulse actuation with $T_p = T_s$ and $T = 2T_p$ (Figure 5). T_s is dependent on the droplet volume. Here, T_p = 2 ms (0.4 μL), 3 ms (1 μL), 5.3 ms (3 μL), 7 ms (5 μL), and 9 ms (10 μL). The period (T) of the square pulse is experimentally determined by monitoring the spreading and receding behaviors of a droplet with respect to the applied voltage. When the applied pulse timing (T_p and T) is well-matched to that of droplet oscillation, the apex height of the detached droplet is increased in the airborne state (see Supporting Information). By using double square pulse actuation, the threshold voltage for 5 μL droplets is reduced to 105−120 V (η = 0.42−0.57), ~20% smaller than the threshold value for a single square pulse actuation (Figure 5). For other volumes of droplets, the threshold voltage for droplet detachment is also reduced by adopting the double square pulse actuation ($T = 2T_p$). This results from the fact that the multiple square pulse actuations increase the up-and-down amplitude of droplet oscillation and reinforce the surface energy of the stretched droplet. Consequently, the multiple pulse actuation method can be used to reduce the threshold voltage for droplet detachment.

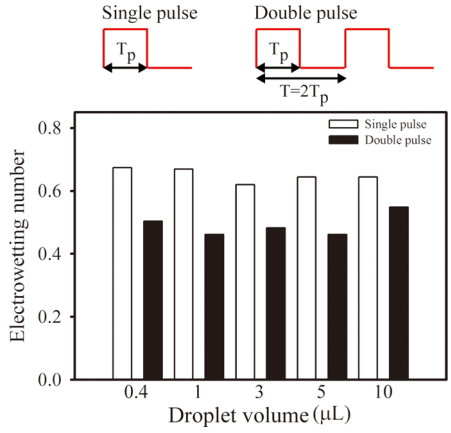

Figure 5. Threshold electrowetting number of droplet detachment at different droplet volumes for single and double square pulse actuation methods. The pulse width T_p is equal to the spreading time T_s, which is dependent on the droplet volume. Here, T_p = 2 ms (0.4 μL), 3 ms (1 μL), 5.3 ms (3 μL), 7 ms (5 μL), and 9 ms (10 μL). The experimental error is typically ±3% of the shown value.

As mentioned above, the threshold voltage for droplet detachment was obtained experimentally. This threshold voltage also can be derived from energy balance between the electrical energy imparted by the applied voltage and the adhesion work. When a sessile droplet spreads to the maximum spread diameter by electrowetting, the energy variation on this transition is the electrical energy. The electrical energy per unit area can be expressed as $E_e = \varepsilon\varepsilon_o V^2/2d$, which is also be given by multiplication of EW number and surface tension. On the other hand, the work required to dewet a sessile droplet from a solid surface is given by adhesion.[33] The adhesion work between the liquid and solid surface is defined as the energy required to separate a flat liquid−solid interface into a liquid−vapor and a solid−vapor interface. It represents the energy required to detach a sessile droplet from a solid surface, which is given by $W_{adh} = \gamma(1 + \cos\theta_Y)$.[33] Here, θ_Y is Young's contact angle of the sessile droplet on a flat solid surface. To detach a droplet from a solid surface, the electrical energy (E_e) applied to the droplet should be larger than the adhesion work (W_{adh}). When $E_e = W_{adh}$, therefore, the threshold EW number

dx.doi.org/10.1021/la404344y | Langmuir 2014, 30, 1805−1811

($\eta_{threshold}$) or threshold voltage ($V_{threshold}$) can be derived as follow:

$$\eta_{threshold} = (1 + \cos\theta_Y) \quad (1)$$

$$V_{threshold} = [2d\gamma(1 + \cos\theta_Y)/\varepsilon\varepsilon_o]^{1/2} \quad (2)$$

For the experimental condition of ε = 3.14, $\varepsilon_o = 8.854 \times 10^{-12}$ Fm^{-1}, $d = 5 \times 10^{-6}$ m, θ_Y = 116°, and γ = 0.072 Nm^{-1}, the above threshold values are estimated to be $\eta_{threshold}$ = 0.57 and $V_{threshold}$ = 123 V. This theoretically predicted threshold is depicted by a short dotted line in Figure 4. The predicted threshold voltage is ~88% of the experimentally measured value. For superhydrophobic surfaces with θ_Y = 160°, theoretical prediction of the threshold voltage is ~40 V, which corresponds to ~67% of the experimental result (60 V).[16] Although the above-mentioned relationships are simply derived by considering only the electrical energy and the adhesion work, they seem to provide the proper scale of threshold for droplet detachment. The relationship also supports the experimental result that the threshold voltage is independent of droplet volume (Figure 4).

Actually, the use of a needle electrode is somewhat inappropriate for 3-D DMF systems. Therefore, we tried to detach a droplet from a solid surface by using interdigitated electrodes (Figure 1b) without utilizing a top needle electrode. When a single square pulse is applied with V_a = 240 V and T_p = 7 ms, 5 μL droplets are not detached from the substrate even at a high value of η = 0.9. Notably, to estimate η for the experimental setup with interdigitated electrodes, the voltage V between the liquid at the contact line and the adjacent electrode beneath the dielectric layer is set to $V_a/2$. In addition, the applied voltage is reduced to ~10% due to the presence of a 20 μm gap between the two comb-shaped electrodes, where electric voltage is not applied.[34]

To find the reason for the undetachable droplet from the substrate with interdigitated electrodes even at high applied voltages, the temporal evolution of the base radius of a droplet was analyzed, according to the parallel and perpendicular directions of the interdigitated electrode substrate (Figure 6). When the orientation is parallel to the electrode axis, the overall spreading motion of a droplet along the direction of the interdigitated electrode is similar to that of a droplet on a flat substrate with a top needle electrode (Figure 2b). Moreover, along this direction, the maximum base radius of spreading droplet (Figure 6b) is similar to that of spreading droplet on a flat substrate with a top needle electrode (Figure 2b). However, when the orientation is perpendicular to the electrode axis, the overall spreading motion of a droplet on this direction contains several consecutive steps. These steps are attributed to the pinning of the contact line along the gaps between two electrodes.[29] In addition, the maximum base radius along the perpendicular direction is smaller than that along the parallel direction (Figure 6c). Consequently, the receding motion of a droplet exhibits large deviation with respect to the orientation of the electrode substrate. From these results, we can see that the nonaxisymmetric spreading motion mainly hinders the detachment of a droplet. The surface energy stored nonaxisymmetrically on the stretched droplet is partially consumed for azimuthal oscillation of the receding droplet. This azimuthal oscillation does not contribute to the droplet detachment. In this case, high surface energy is required to detach droplets from the substrate surface.

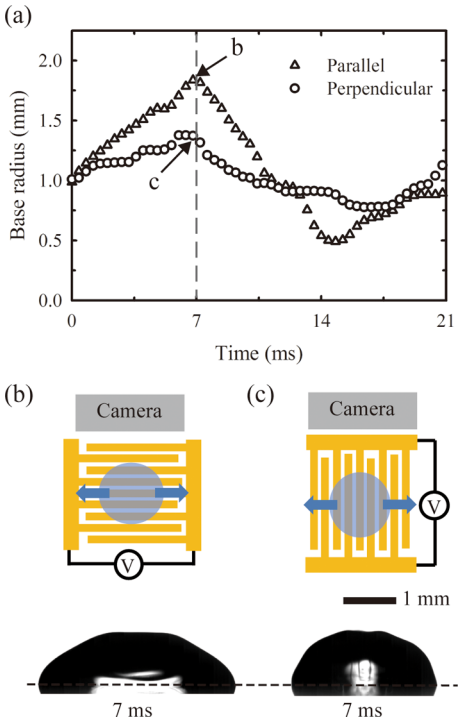

Figure 6. (a) Variation of base radius of a droplet on the bottom surface of interdigitated electrodes in two orthogonal directions at 240 V (η = 0.9) with T_p = 7 ms; one (triangle) is parallel to the electrode length and the other (circle) is perpendicular to the electrode axis. (b) Side-view image of a droplet (5 μL) at maximum spread in the direction parallel to the electrode axis. (c) Side-view image of a droplet (5 μL) at maximum spread in the direction perpendicular to the electrode axis. The base radii of (b) and (c) are denoted in (a) by arrows. In (b) and (c), the dotted lines represent the contact surface of the droplet.

To detach droplets from the surface of interdigitated electrodes, we employed the double square pulse actuation method. As shown in Figure 7, 5 μL droplets can be detached

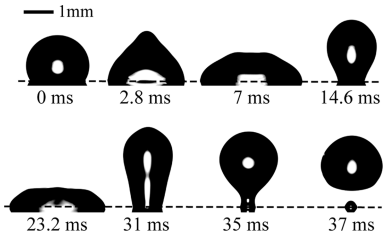

Figure 7. Consecutive side-view images of a 5 μL droplet detached from the bottom surface of interdigitated electrodes by using double square pulse actuation at 240 V (η = 0.9) with T_p = 7 ms and T = ~16 ms. The dotted lines indicate the contact surface of the droplet.

from the bottom surface by applying the double square pulse at 240 V (η = 0.9) with T_p = 7 ms and T = ~16 ms. However, a tiny satellite droplet (diameter of ~450 μm) is formed during the detachment process, which then remained on the bottom substrate (images at 35–37 ms in Figure 7). The small satellite droplet may be caused by the asymmetric spreading motion, as discussed in Figure 6. Although the detachment of a whole droplet from a hydrophobic surface is not complete under this electrode setup, this kind of electrode system would be useful to enhance dropwise condensation heat transfer by massive

dx.doi.org/10.1021/la404344y | Langmuir 2014, 30, 1805–1811

detachment of droplets.[3] In addition, droplets can be easily detached by using this electrode setup, regardless of the droplet position on the bottom electrode.

4. CONCLUSIONS

Electrowetting with a square pulse actuation is applied to detach a droplet from a hydrophobic surface. The threshold condition for detaching droplets from the substrate surface is found to be η = ~0.65 (~130 V), which is almost independent of droplet volume. The threshold value is also theoretically derived by balancing the electrical energy with adhesion work. The theoretical prediction is fairly well-matched with the experimental result. To reduce the threshold voltage for use in practical applications, the double square pulse method is adopted. The threshold voltage for the double square pulse actuation is reduced by ~20% from that for the single square pulse actuation. It is also demonstrated that droplets can be detached effectively from the bottom surface of interdigitated electrodes without using a top needle electrode by employing the double square pulse actuation method. This electrowetting-induced droplet detachment method with interdigitated electrodes system has a strong potential in practical engineering applications, such as enhancement of heat transfer rate with the effective removal of condensate drops from solid surfaces. In addition, the proposed methods would be useful for the construction of 3-D DMF platforms without superhydrophobic surface treatment.

■ ASSOCIATED CONTENT

Ⓢ Supporting Information

Variations of dimensionless jumping height according to the applied voltage for 0.4 μL droplets and comparison of the apex heights of the detached droplet for single and double pulse actuations. This material is available free of charge via the Internet at http://pubs.acs.org.

■ AUTHOR INFORMATION

Corresponding Authors

*Phone: +82-54-279-2273. Fax: +82-54-279-5528. E-mail: iskang@postech.ac.kr.

*Phone: +82-54-279-2169. Fax: +82-54-279-3199. E-mail: sjlee@postech.ac.kr.

Author Contributions

†These authors equally contributed to the work.

Notes

The authors declare no competing financial interest.

■ ACKNOWLEDGMENTS

This work was supported by the National Research Foundation of Korea (NRF) grant funded by the Korea government (MSIP) (no. 2008-0061991). This research was also supported by Career Scientist Program grant no. 2013R1A1A2011956 funded by the Ministry of Science, ICT and Future Planning (MSIP) through the National Research Foundation of Korea (NRF).

■ REFERENCES

(1) Kim, H.-Y. Drop fall-off from the vibrating ceiling. *Phys. Fluids* **2004**, *16*, 474.

(2) Kim, J.; Kaviany, M. Purging of dropwise condensate by electrowetting. *J. Appl. Phys.* **2007**, *101* (10), 103520.

(3) Kim, J.; Kaviany, M. Electrowetting purged surface condensate in evaporators. *Heat Transfer Eng.* **2010**, *31* (2), 101−107.

(4) Robinson, A. K. Vibration-induced droplet atomization and dropwise condensation. University of Florida, Ph.D. Thesis, 2005.

(5) Palan, V.; Shepard, W. S., Jr. Enhanced water removal in a fuel cell stack by droplet atomization using structural and acoustic excitation. *J. Power Sources* **2006**, *159* (2), 1061−1070.

(6) 't Mannetje, D. J. C. M.; Murade, C. U.; van den Ende, D.; Mugele, F. Electrically assisted drop sliding on inclined planes. *Appl. Phys. Lett.* **2011**, *98* (1), 014102.

(7) Yi, U.-C.; Kim, C.-J. Soft printing of droplets pre-metered by electrowetting. *Sens. Actuators, A* **2004**, *114* (2), 347−354.

(8) Pollack, M. G.; Fair, R. B.; Shenderov, A. D. Electrowetting-based actuation of liquid droplets for microfluidic applications. *Appl. Phys. Lett.* **2000**, *77* (11), 1725−1726.

(9) Cho, S. K.; Moon, H.; Kim, C.-J. Creating, transporting, cutting, and merging liquid droplets by electrowetting-based actuation for digital microfluidic circuits. *J. Microelectromech. Syst.* **2003**, *12* (1), 70−80.

(10) Abdelgawad, M.; Freire, S. L.; Yang, H.; Wheeler, A. R. All-terrain droplet actuation. *Lab Chip* **2008**, *8* (5), 672−677.

(11) Fair, R. B. Digital microfluidics: Is a true lab-on-a-chip possible? *Microfluid. Nanofluid.* **2007**, *3* (3), 245−281.

(12) Graham, C.; Griffith, P. Drop size distributions and heat transfer in dropwise condensation. *Int. J. Heat Mass Transfer* **1973**, *16* (2), 337−346.

(13) Choi, K.; Ng, A. H.; Fobel, R.; Wheeler, A. R. Digital microfluidics. *Annu. Rev. Anal. Chem.* **2012**, *5*, 413−440.

(14) Zhao, Y.; Chakrabarty, K. Cross-contamination avoidance for droplet routing in digital microfluidic biochips. *IEEE Trans. Comput.-Aided Des. Integr. Circuits Syst.* **2012**, *31* (6), 817−830.

(15) Yang, H.; Fan, S.-K.; Lin, C.-P.; Wu, C. T.; Hsu, W. 3D droplet transportation by EWOD actuations on flexible polymer films. *ASME Int. Mech. Eng. Congr. Expo.* **2005**, 249−252.

(16) Lee, S. J.; Lee, S.; Kang, K. H. Droplet jumping by electrowetting and its application to the three-dimensional digital microfluidics. *Appl. Phys. Lett.* **2012**, *100* (8), 081604.

(17) Wang, G.; Teng, D.; Fan, S.-K. Three-dimensional digital microfluidics and applications. *7th IEEE Int. Conf. Nano/Micro Eng. Mol. Syst., NEMS* **2012**, 415−418.

(18) James, A.; Vukasinovic, B.; Smith, M. K.; Glezer, A. Vibration-induced drop atomization and bursting. *J. Fluid Mech.* **2003**, *476*, 1−28.

(19) Takeda, K.; Nakajima, A.; Hashimoto, K.; Watanabe, T. Jump of water droplet from a super-hydrophobic film by vertical electric field. *Surf. Sci.* **2002**, *519* (1), L589−L592.

(20) Roux, J.-M.; Fouillet, Y.; Achard, J.-L. 3D droplet displacement in microfluidic systems by electrostatic actuation. *Sens. Actuators, A* **2007**, *134* (2), 486−493.

(21) Lee, S. J.; Lee, S.; Kang, K. H. Jumping of a droplet on a superhydrophobic surface in AC electrowetting. *J. Visualization* **2011**, *14* (3), 259−264.

(22) Kang, K. H. How electrostatic fields change contact angle in electrowetting. *Langmuir* **2002**, *18* (26), 10318−10322.

(23) Mugele, F.; Baret, J.-C. Electrowetting: From basics to applications. *J. Phys.: Condens. Matter* **2005**, *17* (28), R705−R774.

(24) Celia, E.; Darmanin, T.; Taffin de Givenchy, E.; Amigoni, S.; Guittard, F. Recent advances in designing superhydrophobic surfaces. *J. Colloid Interface Sci.* **2013**, *402* (15), 1−18.

(25) Heikenfeld, J.; Dhindsa, M. Electrowetting on superhydrophobic surfaces: Present status and prospects. *J. Adhes. Sci. Technol.* **2008**, *22* (3), 319−334.

(26) Lapierre, F.; Thomy, V.; Coffinier, Y.; Blossey, R.; Boukherroub, R. Reversible electrowetting on superhydrophobic double-nano-textured surfaces. *Langmuir* **2009**, *25* (11), 6551−6558.

(27) Lapierre, F.; Coffinier, Y.; Boukherroub, R.; Thomy, V. Electro-(de)wetting on superhydrophobic surfaces. *Langmuir* **2013**, *29* (44), 13346−13351.

(28) Hong, J.; Kim, Y. K.; Kang, K. H.; Oh, J. M.; Kang, I. S. Effects of drop size and viscosity on spreading dynamics in DC electrowetting. *Langmuir* **2013**, *29* (29), 9118−9125.
(29) Banpurkar, A. G.; Nichols, K. P.; Mugele, F. Electrowetting-based microdrop tensiometer. *Langmuir* **2008**, *24* (19), 10549−10551.
(30) Hong, J.; Lee, S. J.; Koo, B. C.; Suh, Y. K.; Kang, K. H. Size-selective sliding of sessile drops on a slightly inclined plane using low-frequency AC electrowetting. *Langmuir* **2012**, *28* (15), 6307−6312.
(31) James, A. J.; Smith, M. K.; Glezer, A. Vibration-induced drop atomization and the numerical simulation of low-frequency single-droplet ejection. *J. Fluid Mech.* **2003**, *476*, 29−62.
(32) Peykov, V.; Quinn, A.; Ralston, J. Electrowetting: A model for contact-angle saturation. *Colloid Polym. Sci.* **2000**, *278* (8), 789−793.
(33) Israelachvili, J. *Intermolecular and surface forces*; Academic Press: New York, 2010.
(34) Yi, U.-C.; Kim, C.-J. Characterization of electrowetting actuation on addressable single-side coplanar electrodes. *J. Micromech. Microeng.* **2006**, *16* (10), 2053−2059.